Available online at www.sciencedirect.com

jmr&t Journal of Materials Research and Technology

journal homepage: www.elsevier.com/locate/jmrt

Original Article

Compressive performance of fiber reinforced polymer encased recycled concrete with nanoparticles

Chang Gao [a], Liang Huang [a,**], Libo Yan [b,c,*], Bohumil Kasal [b,c], Wengui Li [d], Ruoyu Jin [e], Yutong Wang [a], Yin Li [a], Peng Deng [a]

[a] Key Laboratory for Green and Advanced Civil Engineering Materials and Application Technology of Hunan Province, College of Civil Engineering, Hunan University, Changsha 410082, China
[b] Centre for Light and Environmentally-Friendly Structures, Fraunhofer Wilhelm-Klauditz-Institut WKI, Bienroder Weg 54E, Braunschweig, 38108, Germany
[c] Department of Organic and Wood-Based Construction Materials, Technische Universität Braunschweig, Hopfengarten 20, 38102 Braunschweig, Germany
[d] School of Civil and Environmental Engineering, University of Technology Sydney, NSW 2007, Australia
[e] School of Built Environment and Architecture, London South Bank University, 103 Borough Rd, London, SE1 0AA, UK

ARTICLE INFO

Article history:
Received 27 April 2021
Accepted 31 July 2021
Available online 8 August 2021

Keywords:
Recycled concrete
Waste cracked brick aggregates
Fiber reinforced polymer (FRP)
Nanoparticles
Axial compressive performance

ABSTRACT

Nanomaterials have been used in improving the performance of construction materials due to their compacting micro-structure effect and accelerating cement hydration reaction. Considering the brittle characteristic of fiber reinforced polymer (termed as FRP) tube encased concrete and inferior properties of recycled concrete, nanoparticles were used in FRP tube encased recycled aggregate concrete. The axial compressive performance of FRP tube used in recycled concrete treated with nanoparticles strengthening, termed as FRP-NPRC, were investigated by axial compression experiments and theoretical analysis. Five experimental variables were considered including (1) the dosages and (2) varieties of nanoparticles (i.e. 1% and 2% of nanoSiO_2, 1% and 2% of nano$CaCO_3$), (3) replacement ratios of recycled coarse aggregates (termed as RCAs) (0%, 50%, 70% and 100%) the RCAs were mainly produced from the waste cracked bricks, (4) the number of glass FRP (GFRP) tube layers (2, 4 and 6-layer) and (5) the mixing methods of concrete. Results indicate that the combination of FRP confinement and nanoparticle modification in recycled concrete exhibited up to 76.2% increase in compressive strength and 7.62 times ductility improvement. Furthermore, a design-oriented stress–strain model on the basis of the ultimate condition analysis were executed to evaluate the stress–strain property of this strengthened component.

* Corresponding author.
** Corresponding author.
E-mail addresses: lianghuanghnu@gmail.com (L. Huang), l.yan@tu-braunschweig.de, libo.yan@wki.fraunhofer.de (L. Yan).
https://doi.org/10.1016/j.jmrt.2021.07.159

1. Introduction

The urbanization process led to a massive amount of constructional waste. Considering environmental conservation, natural resources reserve and land occupation, promoting the application and recycling of construction waste has been urgent appealing [1–4]. In recent years, recycling construction materials for new application such as recycled aggregate concrete has shown commercial, environmental and technical benefits. In practice, recycled aggregates are primarily obtained from old concrete rubbles, waste masonry and other kinds of construction waste (e.g., glass and wooden debris) [5–7]. While most researches mainly focused on recycled concrete mixed with relatively homogenous laboratorial recycled aggregates [7], and researchers unanimously agree on the high-cost and technically impossible implement of the full sorting and screening of recycled aggregates in practice. However, the actual recycled aggregate mixture generally exhibited different physical and mechanical characteristics than the homogenous recycled aggregates or natural aggregates, e.g., higher porosity and water absorption, impermeability, complex constitution, lower compressive strength and concerned durability [8,9], e.g., the crushing index of recycled aggregates can be 1.5 times that of natural aggregates, and the moisture ratio can even reach 7 times. The high moisture ratio and porosity of recycled aggregates produced from waste bricks could lead to the poor performance of the resulting recycled aggregate concrete such as reduction in strength and stiffness, increased creep and shrinkage [10]. Besides, the diversification of construction waste sources and the complex contents of recycled aggregates would cause the dispersion and uncertainty in fluidity, mechanical properties and durability of the resulted recycled concrete [11]. In addition, the technology on recycled aggregates production and excessive classification could result in several flaws as energy consumption, complicated operation, and overmuch cost and labor supplement [12]. Overall, it is necessary to find economically effective and maneuverable approaches to widen the application of recycled concrete considering the social and environmental benefits.

Concrete is one non-homogeneous material whose characteristics closely rely on the behavior of each single constitute, e.g., mixing water, aggregate, cement matrix, admixtures and even the Interfacial Transition Zones (ITZs) of concrete interior [13–15]. ITZs are defined as the boundary region among different materials in a composite and the ITZs in the concrete mixtures are normally regarded as the lowest-strength part compared to those of the aggregates and the mortar matrix, where normally leads to the rupture of concrete. Generally, the ITZs, the content of the old mortar was considered as significant influencing indexes of the properties of the recycled concrete [13–17]. The recycled aggregates exhibit more complex composition than the natural aggregates because there is old mortar attached to the surface of recycled aggregates. Thus, compared to natural aggregate concrete, more types of ITZs in recycled concrete can be found at their micro-structural level observation, as shown in Fig. 1, i.e. one old ITZ between the prior aggregate and the adhesion mortar, another two new ITZs including one boundary between the prior aggregate and the fresh mortar, and another boundary between the old attached mortar and the fresh mortar [15]. The new ITZs formed in the mixing and vibrating process of the recycled aggregate concrete mixture. Against this background, recent researchers considered using different mixing approaches to improve the ITZs. Two-Stage Mixing Approaches (TSMAs) was proposed to renovate the ITZs [14,18–20]. The TSMA was achieved by firstly mixing the recycled aggregates and cement together, and then adding natural aggregates and stirring. The TSMA functioned in concrete promotion by forming a layer of cement paste covering recycled aggregates, filling up initial damage of recycled aggregates and improving the ITZs [14].

Nanomaterials, as defined as materials in nanometers, have been used with conventional construction materials and achieved superior properties of concrete. In previous studies, several types of nanomaterials have been used in the construction materials, e.g., nanoSiO_2 (NS) [21–25], nano-limestone (NL) [25], nanoTiO_2 (NT) [26], nano$CaCO_3$ (NC) [27], carbon nanotubes (CNT) [28–30], etc. Improvements on concrete have been found by using nanomaterials as promoted strength and the durability [22–26,31], accelerated the hydration reaction and dense micropores [24–30], and densified ITZs between the aggregates and the cement paste [31,32]. Studies have shown that the addition of nanomaterials, e.g. nanoSiO_2 and nano-limestone leads to strength enhanced conventional concrete [33,34]. Recent research also showed that the nanoparticles (e.g., nanoSiO_2, nano$CaCO_3$ and nano-limestone, etc.) could act on improving the porous microstructure and mechanical properties of recycled concrete [22,31,32,35,36]. Studies of Li et al. indicated that the nanoSiO_2 was more efficient on the mechanical strength advance of

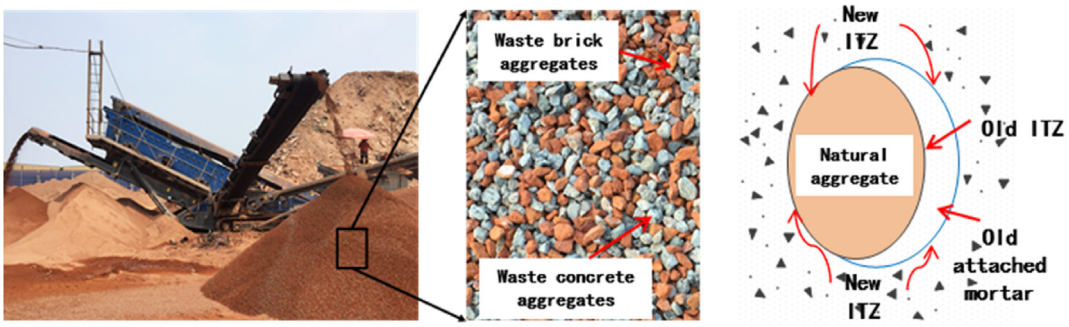

Fig. 1 – Schematic instruction of ITZs in recycled concrete.

Table 1 – Physical property of aggregates.

Types	Partial size (mm)	Density (kg/m^3)	Porosity (%)	Water absorption (%)	Moisture content (%)	Crushing index (%)
RCAs	5–10	1140	10	14.8	6.5	17.3
NCAs	5–10	1620	6	1.7	0.3	10.7
FAs	0.5–0.25	1450	12	–	3.0	–

recycled concrete than the nano-limestone, and the porosity of recycled concrete treated with nanoSiO_2 reduced remarkably [35]. Bibhuti et al. confirmed the positive effect of nanoSiO_2 admixture on recycled concrete by fundamental mechanical tests, the Rebound Number and Ultrasonic Pulse Velocity based on the Non-Destructive tests demonstrated that concrete mixtures containing nanoSiO_2 acquired the reduction of voids and denseness of the concrete mixture with relative strength compared with the controlling natural concrete counterpart [36].

Lateral confined concrete has been diffusely authorized to realize superior structures and constructions [37–43]. Fiber reinforced polymer (FRP) composites such as traditional synthetic and other innovative FRP materials, i.e., basalt FRP (BFRP) [46], flax FRP (FFRP) [47] and polyester FRP (PFRP) [48–50], as one superior concrete strengthened mode, have been studied and applied popularly. Recent studies conducted the performance of FRP strengthening recycled concrete [44–50]. Our research group has compared the compressive behavior of synthetic FRP, natural fibers and textile encased recycled concrete and indicated the remarkable promotion of FRP on compressive resistance of recycled concrete [44,47–50]. Ozbakkaloglu et al. [46] concluded the impacts of recycled aggregate replacement rate, column cross-section shape (i.e. circular cross-section vs. square cross-section) and FRP type on FRP strengthening recycled concrete under compression.

In this study, the compressive performance of GFRP encased recycled concrete treated with nanoparticles was experimentally and theoretically investigated. The admixture of nanoparticles serves in compacting recycled concrete micro-structure and filling the voids of aggregates, accelerating hydration reaction, resulted remarkable workability and performance, increasing pozzolanic action and strengthening the ITZs. The admixture of nanoparticles could lead to superior mechanical performance and promising durability of recycled concrete. Specifically, the objectives of this work included:

(a) To obtain the axial compressive properties of GFRP encased recycled concrete treated with nanoparticles.
(b) To investigate the influences of dosages and types of nanoparticles (1% and 2% of NS, 1% and 2% of NC), replacement ratios of RCAs in recycled concrete (0%, 50%, 70% and 100%), the thickness of GFRP tubes (2, 4 and 6-layer glass fiber thickness) and the mixing methods of concrete on the performance of FRP encased recycled concrete treated with nanoparticles under compression;
(c) To validate the ultimate conditions and stress–strain models to stimulate the stress–strain response of FRP encased recycled concrete treated with nanoparticles.

Table 2 – Physical properties of nanoSiO_2.

	Appearance	Density (g/cm^3)	Size (mm)	PH	Price/kg
nanoSiO_2	White powder	1.1–1.2	8–15	8–9.5	$29.6

2. Experiments

2.1. Materials and preparation

2.1.1. Classification and tests on aggregates

The RCAs used in this study were a mixture from 55 wt.% fireclay brick waste and 45 wt.% of waste concrete rubbles. The RCAs were directly produced industrially and used in the tests without additional sorting process for validating the practicability of test samples in actual engineering. Table 1 shows the details of aggregates. The crushing index of RCAs was achieved the demands of Standard GB/T 25177-2010 [51]. Cement of P.O. 42.5 and fine aggregates (FAs) with fineness modulus of 2.57 were used in mixture of the concrete.

2.1.2. Nanoparticles

The physical details of nanoSiO_2 (NS) and nano$CaCO_3$ (NC) in respective Tables 2 and 3 were provided by the manufacturers. As well known, the insufficient dispersing or deagglomeration of nanoparticles in nanoparticle liquid fabrication could result in inferior concrete properties, e.g. pre-exiting micro-cracks, partial stress-concentration [34,35]. Thus, the surfactant of Gum Arabic (GA) was used to promote the dispersion of nanoparticles in this study. The GA could separate the nanoparticles and promote the nanoparticles dissolution by wrapping around the nanoparticles and preventing the attraction of nanoparticles [35]. The weight ratio of NS or NC and GA was 1:6 according to the instructions of GA usage. The GA was firstly diluted with some water, then the NS or NC was added into the dilution and mixed until the mixture was visually uniform and no aggregation.

2.1.3. GFRP

The unidirectional glass fibers were used to fabricate the GFRP tubes. Tensile tests of GFRP laminates were executed to obtain the experimentally relevant parameters of GFRP [52]. The test average elastic modulus, tensile strength, and ultimate strain of single lamina GFRP laminate were 60.6 GPa, 956 MPa, and 1.60%, respectively.

Table 3 – Physical properties of $nanoCaCO_3$.

	Appearance	Density (g/cm^3)	Size (mm)	PH	Price/kg
$nanoCaCO_3$	White powder	2.5–2.6	15–40	8–9	$33.3

2.1.4. *Fabrication of specimens*

The GFRP tubes was prefabricated by a typical hand lay-up process as expressed in a previous study [44]. Table 4 expressed the mix proportions of core recycled concrete. The fresh recycled concrete treated with nanoparticles was casted in two different two-stage mixing approaches, i.e., MI and MII. For the first mixing methods, namely MI, the NS or NC admixture was firstly mixed with RCAs and half mixing water, then mixed with the cement, fine aggregates and the rest of mixing water. For the second method, namely MII, the cement, sand and RCAs were firstly dryly mixed, then all water was added and stirred until uniform. Finally, the NS or NC admixture was poured into the fresh concrete mix and stirred for 90s. The mixed concrete was poured into prefabricated GFRP tube and vibrator-stirred for 30s. All casted specimens were conserved in the normal concrete curing room for 28 days.

2.2. *Test matrix*

To explore the performance of GFRP-recycled concrete treated with nanoparticles under axial compression, 63 cylindrical specimens (i.e. 12 untreated plain recycled concrete specimens, 18 recycled concrete specimens treated with nanoparticles and 33 GFRP encased recycled concrete treated with nanoparticles specimens) were constructed and tested under axial compressive load, as shown is Table 5. The dimensions of specimens were diameter $\times$ height $= 100 \times 200$ mm^2. Test variables included the types of nanoparticles (i.e., $nanoSiO_2$ and $nanoCaCO_3$) and the weight ratios of nanoparticles (1% and 2% of $nanoSiO_2$, 1% and 2% of $nanoCaCO_3$), the thickness of GFRP tubes (2, 4 and 6-layer glass fiber thickness), the replacement rates of RCAs (i.e., 0%, 50%, 70% and 100%), two kinds of TSMAs of fresh concrete treated with nanoparticles (i.e., MI and MII as discussed in details in Section 2.1.4). These specimens were classified into untreated plain concrete specimen categories, 6 categories of nanoparticles modified specimens and 11 categories of glass fibre reinforced polymer encased nanoparticles modified specimens (termed as GFRP-NSRC or GFRP-NCRC, respectively). Each category consisted of three identical specimens. For untreated plain recycled concrete specimens, the capital letters PC denoted the untreated concrete specimens without both nanoparticle modification and FRP confinement, the capital letter A with a figure denoted the replacement ratios r of RCAs. For un-encased recycled concrete specimens treated with nanoparticles, the capital letters NS and NC denoted the types of nanoparticles as $nanoSiO_2$ and $nanoCaCO_3$, respectively, the capital letter A with a digit also denoted the replacement ratios r of RCAs, the capital letter M with a Roman digit denoted the mixing methods of fresh concrete (i.e., MI and MII). For GFRP encased recycled concrete treated with nanoparticles specimens, the capital letter G followed by a digit denoted the number of glass fiber lamina, and the latter letters and digits denoted the same meaning as those of recycled concrete specimens treated with nanoparticles, e.g., the specimen code G4NS1A70MII denoted GFRP tube encased $nanoSiO_2$ modified recycled concrete specimens with 4 layers of GFRP, 1wt.% of $nanoSiO_2$, 70% replacement ratio of RCAs and the second mixing method of fresh concrete.

2.3. *Experimental tests*

All specimens were loaded under the pressing machine of capacity of 20,000 kN in Fig. 2(a). The load rates were maintained 0.20 mm/min. As illustrated in Fig. 2(b), 10 strain gages with each length of 20 mm, as four longitudinal strain gages (i.e., SG1-4) and four horizontal strain gages (i.e., SG5-8), were stick on the middle height of the specimens, and another two longitudinal strain gages were stick on both ends of specimens (i.e., SG9 and SG10), respectively. Four linear variable differential transformers (LVDTs) were set to record vertical deformation and applied load was recorded by one Material Test System (MTS) and inserted in the compression machine. The data from the strain gages and applied load were measured by the statical strain indicator simultaneously.

3. Experimental results

3.1. *Failure mode*

For all the untreated recycled concrete, NSRC and NCRC specimens without FRP protection, the failure modes were similar that the ruptured with numerous vertical cracks at the external surface of cylinders, but the NSRC or NCRC specimens exhibited shorter cracks than the untreated recycled concrete as Fig. 3(a) and (b). The FRP encased specimens under different variables also exhibited similar failed patterns. The external GFRP tube ruptured around the mid-height of specimens with many transverse teared fibers and the internal concrete crushed down thoroughly. While with a decrease of the numbers of GFRP layers, the external GFRP tube presented more severe ruptured plane with more teared lateral fiber strands and the ruptured plane tended to be higher than the mid-height of cylinders, e.g., the ruptured zone of specimens G2NS1A70MII occurred around the quarter height near the load position, while for specimen G4NS1A70MII and G6NS1A70MII, the ruptured zone tended to occur around the mid-height of cylinders. The possible reason was that the higher stiffness of external GFRP tube with thicker GFRP tube led to the easement of premature failure at the top end of cylinders where most closed to the load position.

3.2. *Stress–strain response*

The typical stress–strain responses of GFRP encased recycled concrete treated with nanoparticles are demonstrated in Fig. 4. The compressive stress–strain response including the

Table 4 – Core concrete mix proportions.

No.	Water (kg/m^3)	Cement (kg/m^3)	Nanoparticles type	Nanoparticles (kg/m^3)	NFA (kg/m^3)	NCA (kg/m^3)	RCAs (kg/m^3)	Mixing method	r
1	121	296	NS	2.96	280	568	0	II	0%
2	121	296	NS	2.96	280	284	284	II	50%
3	121	296	NS	2.96	280	170	398	II	70%
4	121	296	NS	2.96	280	0	568	II	100%
5	121	296	NS	5.92	280	170	398	II	70%
6	121	296	NS	2.96	280	170	398	I	70%
7	121	296	NC	2.96	280	170	398	II	70%
8	121	296	NC	5.92	280	170	398	II	70%
9	121	296	NC	2.96	280	170	398	I	70%

primal parabolic ascending stage (i.e., core recycled concrete treated with nanoparticles bearing stage) and the gentle ascending stage (i.e., activated passive FRP confinement bearing stage) connected with one cambered interim stage.

4. Discussion

4.1. *Harden strength*

The main tested results in this work are listed in Table 6, where f_{co} and ε_{co} are the compressive strength and corresponding axial strain of plain recycled concrete treated with nanoparticles specimens without FRP confinement, respectively, ε_{fu} and $\varepsilon_{fu,a}$ are the ultimate tensile strain of FRP from the material properties tests and actual encased cylindrical specimens, respectively, f_{cc} and ε_{cu} are the compressive strength and ultimate axial strain of the GFRP encased specimens treated with nanoparticles. The skeleton of stress–strain response was achieved as Fig. 5. The transition zone was simplified as the yielding point corresponding to the f_{co} and ε_{co} point. The strength harden ratio is expressed as the ratio of peak strength and yielding strength f_{cc}/f_{co} μ is the ductility index which was calculated as the $\varepsilon_{cu}/\varepsilon_{co}$. f_l is the lateral pressure of external FRP calculated as Eq. (1). The confinement ratio is expressed as f_l/f_{co}.

$$f_l = \frac{2f_{frp}t_{frp}}{d} = \frac{2E_{frp}t_{frp}\varepsilon_{frp,l}}{d} \quad (1)$$

The compressive strength and corresponding axial strain of plain untreated recycled concrete specimens, i.e., PCA0, PCA50, PCA70 and PCA100, are 35.9 MPa and 0.20%, 35.6 MPa and 0.22%, 31.7 MPa and 0.21%, 30.3 MPa and 0.24%, respectively. And the admixture of nanoparticles promoted the mechanical performance of recycled concrete compared with plain untreated specimens.

The GFRP encased recycled concrete specimens treated with nanoparticles showed more remarkable enhancement on the compressive strength compared to corresponding unencased recycled concrete specimens treated with nanoparticles. It is obvious that the strength increased with a thicker FRP tube, i.e., the compressive strength of

Table 5 – Test matrix of the specimens.

No.	Specimens	r of RCAs (%)	Number of GFRP layer n_f	Type of nanoparticles	Weight ratio of nanoparticles (%)	Mixing methods
1	PCA0	0	–	–	–	–
2	PCA50	50	–	–	–	–
3	PCA70	70	–	–	–	–
4	PCA100	100	–	–	–	–
5	NS1A70MII	70	–	nanoSiO_2	1	II
6	NS2A70MII	70	–	nanoSiO_2	2	II
7	NS1A70MI	70	–	nanoSiO_2	1	I
8	NC1A70MII	70	–	nano$CaCO_3$	1	II
9	NC2A70MII	70	–	nano$CaCO_3$	2	II
10	NC1A70MI	70	–	nano$CaCO_3$	1	I
11	G4NS1A0MII	0	4	nanoSiO_2	1	II
12	G4NS1A50MII	50	4	nanoSiO_2	1	II
13	G4NS1A70MII	70	4	nanoSiO_2	1	II
14	G4NS1A100MII	100	4	nanoSiO_2	1	II
15	G2NS1A70MII	70	2	nanoSiO_2	1	II
16	G6NS1A70MII	70	6	nanoSiO_2	2	II
17	G4NS2A70MII	70	4	nanoSiO_2	2	II
18	G4NS1A70MI	70	4	nanoSiO_2	1	I
19	G4NC1A70MII	70	4	nano$CaCO_3$	1	II
20	G4NC2A70MII	70	4	nano$CaCO_3$	2	II
21	G4NC1A70MI	70	4	nano$CaCO_3$	1	I

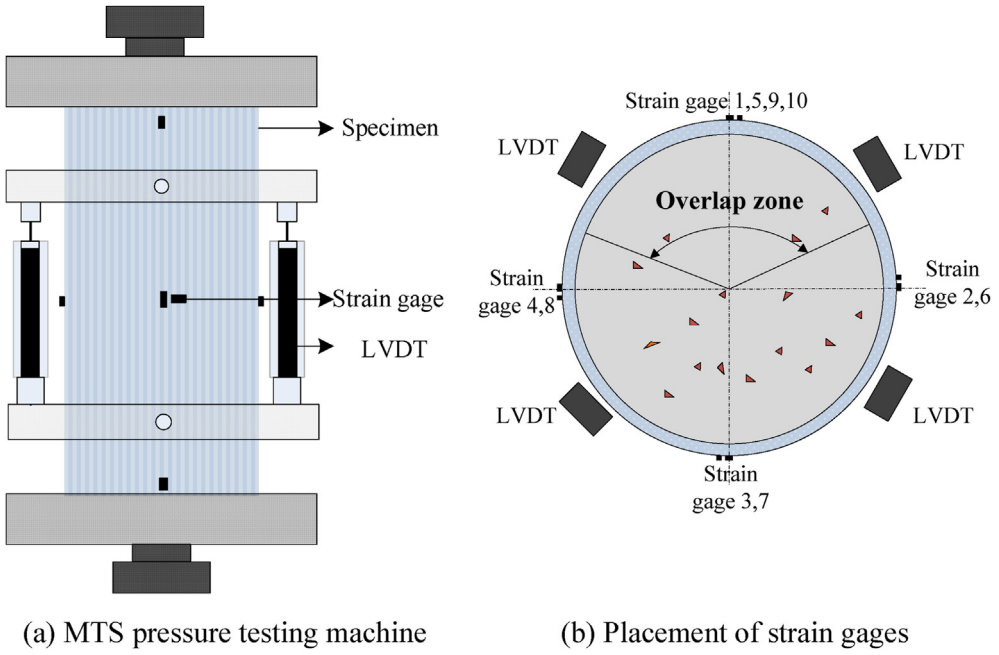

Fig. 2 – Test instrumentation and deformation measurement.

G2NS1A70MII, G4NS1A70MII and G6NS1A70MII specimens was 73.3 MPa, 124.6 MPa and 154.8 MPa, respectively. The compressive strength reduced with more quantities of RCAs, e.g., the specimens with replacement ratios of RCA r = 0% and 100% (i.e., G4NS1A0MII and G4NS1A100MII specimens) presented strength of 142.0 MPa and 111.5 MPa, respectively. Besides, specimens with an increase in the dosage of NS (up to 2wt.% in this study) or the mixing method II exhibited higher enhancement on the compressive strength, while the GFRP-NCRC specimens showed the opposite trend under the effect of dosages of NC or concrete mixing method. The GFRP confined RAC specimens with NS treatment had more strength gain than GFRP confined RAC specimens with NC treatment.

4.2. *Ductility*

The ductility indexes of all GFRP encased recycled concrete treated with nanoparticles specimens and the GFRP encased recycled concrete tested in our previous study [44] were given and compared in Fig. 6. All encased specimens showed significant improvement in the ductility of recycled concrete, the GFRP encased recycled concrete treated with nanoparticles specimens exhibited higher ductility indexes than corresponding GFRP encased recycled concrete with the same replacement ratio of RCAs and thickness of GFRP tube. The ductility index of GFRP encased recycled concrete nanoparticle specimens showed the ascending trend with more quantities of RCAs, while GFRP encased recycled concrete showed the contrary trend. The assumed reasons could be the better filling effect of nanoparticles on the RCAs which were more polyporous than natural aggregates [35]. The ductility index of GFRP encased recycled concrete treated with nanoparticles also increased with thicker FRP tube. The GFRP confined RAC with 1 wt.% and 2 wt.% of nano-SiO_2 treatment specimens show similar ductility nature. The GFRP confined RAC specimens with NS treatment presented lower ductility index with the mixing method I than that of the controlled specimens with the mixing method II. The ductility index of GFRP confined RAC specimens with NC treatment increased slightly with more quantities of nano$CaCO_3$ usage while the two different mixing methods had no significant effect on ductility index of GFRP-NCRC specimens. The GFRP confined RAC specimens with NC treatment exhibited higher ductility index under the MI mixing method compared to the corresponding GFRP confined RAC specimens with NS treatment, while exhibited lower ductility index under the MII mixing method.

4.3. *Ultimate condition*

Two key indexes of FRP encased concrete as the strength and ultimate strain are necessary for describing and determining the ultimate condition. The strength and ultimate strain are concerned with many variables. Numerous strength and strain models have been literately proposed [38,39,53–58], and based on the review of these confinement models, the most common formula of strength model is:

$$\frac{f_{cc}}{f_{co}} = 1 + k_1\left(\frac{f_l}{f_{co}}\right)^{m_1} \tag{2}$$

k_1 and m_1 are the coefficients of the formula, f_l is the lateral pressure, which can be calculated as Eq. (1). To simplify the impact of nanoparticles admixture on the strength, the f_{co}

Fig. 3 – Failure patterns.

used in the equations is the compressive strength of corresponding recycled concrete treated with nanoparticles. The strength model of GFRP encased recycled concrete treated with nanoparticles was regressed and expressed as below:

$$\frac{f_{cc}}{f_{co}} = 1 + 3.28 \times \left(\frac{f_l}{f_{co}}\right)^{0.81} \tag{3}$$

where $k_1 = 3.28$, and $m_1 = 0.81$. The regression analysis curve was shown in Fig. 7.

Based on the discussion above, the model of ultimate strain ε_{cc} of FRP encased recycled concrete treated with nanoparticles specimens was proposed in this section. The glass FRP confined concrete specimens in this study exhibited the monotonically ascending bilinear stress–strain behaviour, and the strains at the peak stress ε_{cc} were equal to the ultimate axial strain ε_{cu}. Generally, the ultimate axial strain is related to the lateral confining stress f_l [53–58]. The model of ultimate strain of FRP encased concrete is expressed as Eq. (4):

$$\frac{\varepsilon_{cc}}{\varepsilon_{co}} = a + k_2\left(\frac{f_l}{f_{co}}\right)^{m_2} \tag{4}$$

where a, k_2 and m_2 are the coefficients of the formula, ε_{co} is equal to the ultimate strain of plain concrete, ε_l is the transverse strain of FRP, the ratio $\varepsilon_{cc}/\varepsilon_{co}$ was called as the strain harden ratio and the ratio f_l/f_{co} was called as the confinement ratio. The model of ultimate strain was regressed with experimental results and the Eq. (4). The regressed strain model was shown as Eq. (5) and the relationship between

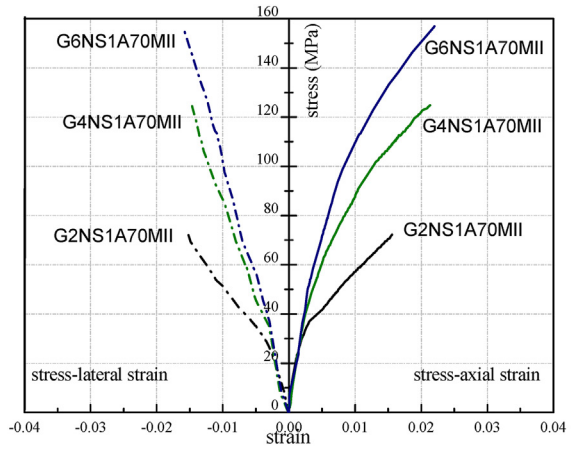

(a) GFRP-NSRC with different stiffness of GFRP

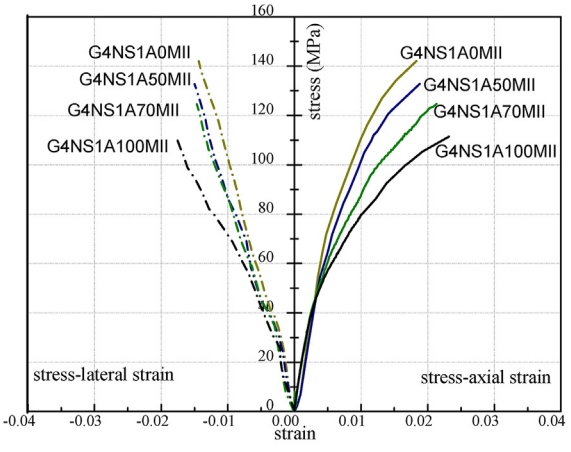

(b) GFRP-NSRC with different replacement ratios of Ras

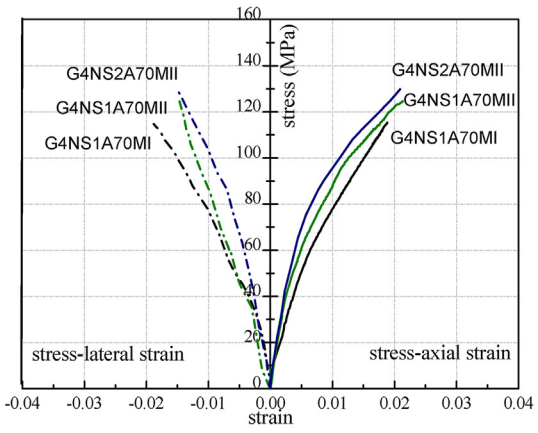

(c) GFRP-NSRC with different dosages of NS and mixing methods

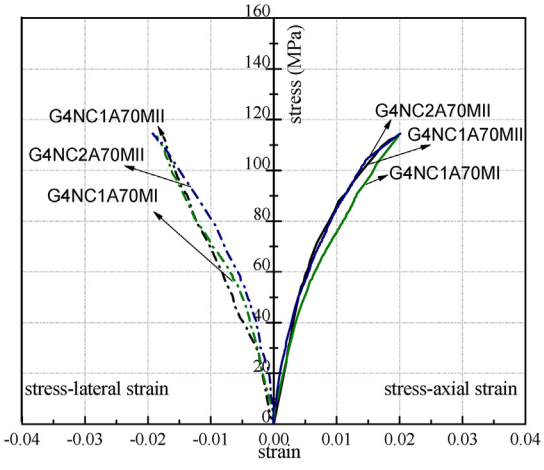

(d) GFRP-NCRAC with different dosages of NC and mixing methods

Fig. 4 – Axial stress–strain curves of GFRP-NSRC and GFRP-NCRC.

strain harden ratio $\varepsilon_{cc}/\varepsilon_{co}$ and confinement ratio f_l/f_{co} was expressed as Fig. 8.

$$\frac{\varepsilon_{cc}}{\varepsilon_{co}} = 4.82 + 3.51 \times \left(\frac{f_l}{f_{co}}\right)^{1.19} \quad (5)$$

4.4. *Stress–strain theoretical models*

The FRP encased recycled concrete with nanoparticles exhibited stress–strain response could be simplified as Fig. 8, containing one parabolic stage followed another straight rising stage. Similar stress–strain response has been reported in existed literature. More amount of nanoparticles admixture increased the slope of the hardening stage and initial stage. The stress–strain model considering the impact of nanoparticles could be applied in the description of the structural behaviour of FRP encased recycled concrete with nanoparticles.

For this kind of stress–strain behaviour, existed stress–strain models for traditional FRP strengthened

Table 6 – Tested results.

Specimens	f_{co} (MPa)	$\varepsilon_{co}(10^{-2})$	$\varepsilon_{fu}(10^{-2})$	f_l (MPa)	f_l/f_{co}	f_{cc} (MPa)	f_{cc}/f_{co}	$\varepsilon_{cu}(10^{-2})$	$\varepsilon_{fu,a}(10^{-2})$	μ
G4NS1A0MII	39.8	0.26	1.60	24.0	0.80	142.0	3.56	1.83	1.41	7.04
G4NS1A50MII	37.6	0.27	1.60	24.0	0.90	132.8	3.53	1.88	1.41	6.96
G4NS1A70MII	36.9	0.29	1.60	24.0	0.86	124.6	3.37	2.13	1.41	7.34
G4NS1A100MII	35.4	0.30	1.60	24.0	0.92	111.5	3.15	2.32	1.41	7.73
G2NS1A70MII	36.9	0.29	1.60	9.3	0.35	73.3	1.98	1.56	1.31	5.38
G6NS1A70MII	36.9	0.29	1.60	33.3	1.25	154.8	4.19	2.46	1.53	8.48
G4NS2A70MII	37.5	0.29	1.60	24.0	0.76	129.8	3.46	2.09	1.41	7.21
G4NS1A70MI	36.1	0.29	1.60	24.0	0.92	115.2	3.19	1.88	1.41	6.48
G4NC1A70MII	34.4	0.28	1.60	24.0	0.98	113.2	3.29	1.94	1.41	6.93
G4NC2A70MII	39.3	0.28	1.60	24.0	0.82	114.9	2.93	2.01	1.41	7.18
G4NC1A70MI	33.8	0.28	1.60	24.0	1.00	113.5	3.35	1.98	1.41	7.07

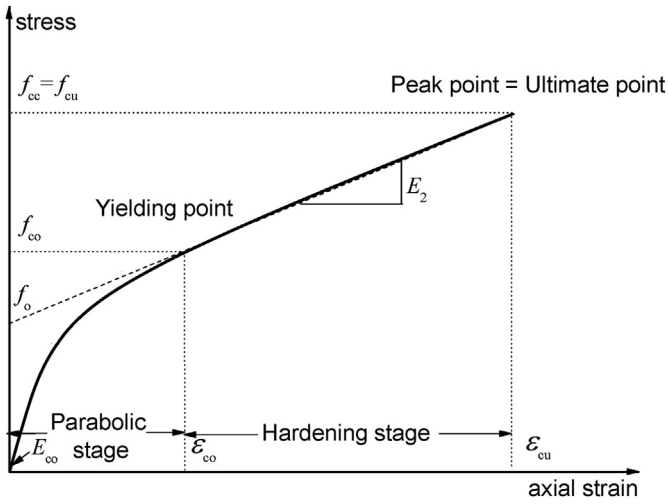

Fig. 5 – Schematic curve of σ –ε general response.

concrete have clear definition of stress–strain response. The design-oriented stress–strain prediction formula raised by Lam and Teng [59] was cited and modified in this part to figure out the stress–strain response of FRP encased recycled concrete treated with nanoparticles. The stress–strain model was generally expressed as below:

$$\sigma_c = E_{co}\varepsilon_c - \frac{(E_{co}-E_2)^2}{4f_o}\varepsilon_c^2 \quad \text{for} \quad 0 \le \varepsilon_c \le \varepsilon_t \tag{6}$$

and

$$\sigma_c = f_o + E_{cc}\varepsilon_c \quad \text{for} \quad \varepsilon_t \le \varepsilon_c \le \varepsilon_{cu} \tag{7}$$

where f_o is the intercept of the stress axis by the hardening stage and taken as the ultimate strength of treated concrete without FRP confinement f_{co} in this situation. The model was established on the assumption that the first and second stages were connected smoothly (i.e., the transition stage was considered as a point called yielding point and no change of the slope happened between two stages). The f_{cc} and ε_{cc} can be calculated as Eqs. (3) and (5). The strain at the yielding point is defined as ε_t:

$$\varepsilon_t = \frac{2f_o}{E_{co}-E_2} \tag{8}$$

where E_2 is the slope of the hardening stage:

$$E_2 = \frac{f_{cc}-f_{co}}{\varepsilon_{cu}} \tag{9}$$

After the determination of each coefficient, the contrast between the experimental and simulative data on the specimens G4NS1A70MII and G4NS2A70MII was executed in Fig. 9. The predicted stress–strain curves correspond to the curves of G4NS1A70MII-M and G4NS2A70MII-M. The stress–strain curves of the determined models well agreed with the test data, confirming the applicability and accuracy of the ultimate condition and stress–strain models.

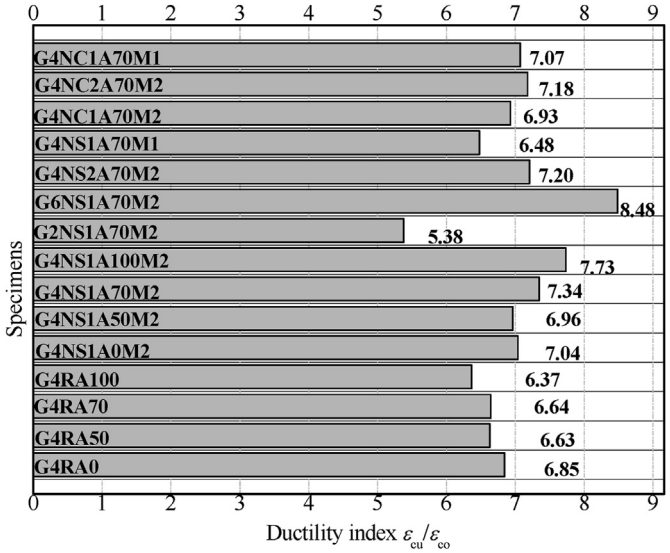

Fig. 6 – Ductility indexes of the GFRP encased specimens.

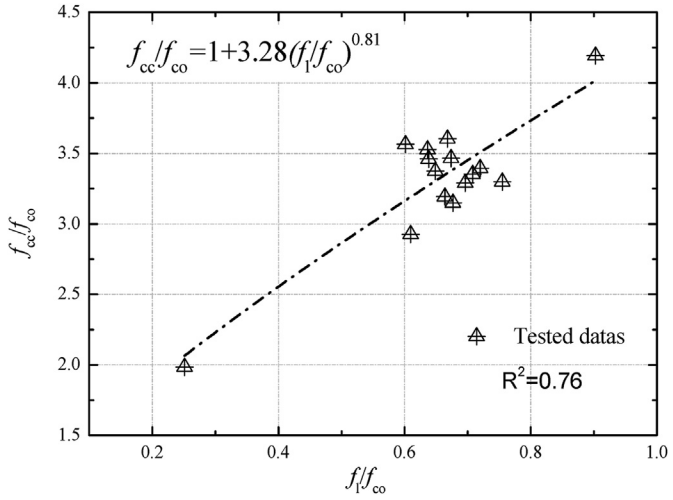

Fig. 7 – Relationship between confinement ratio and strength harden ratio.

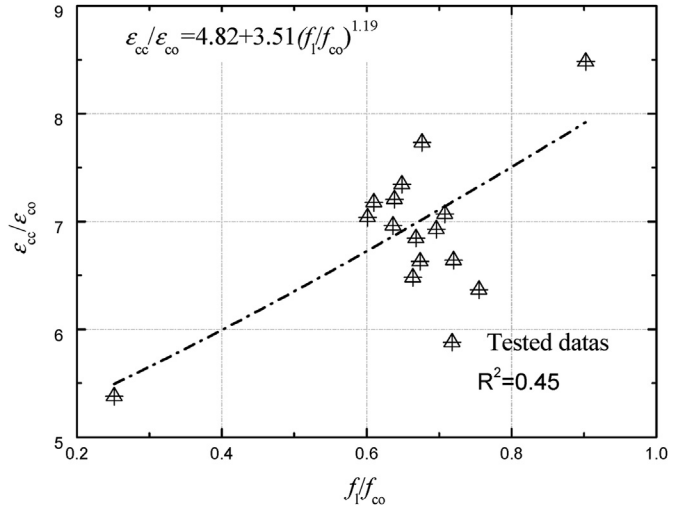

Fig. 8 – Relationship between confinement ratio and strain harden ratio.

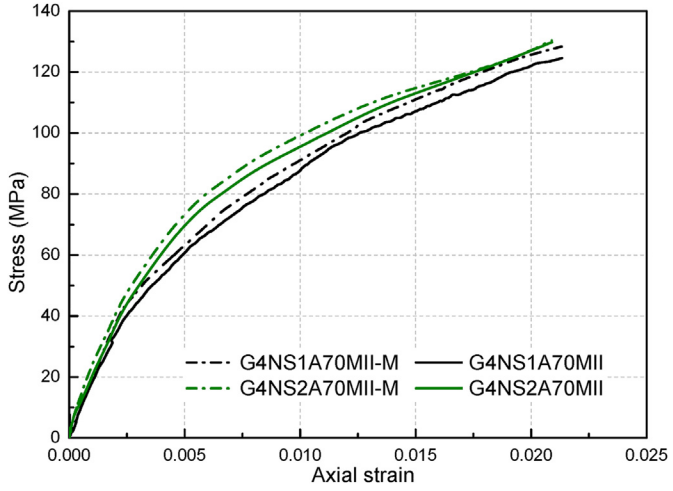

Fig. 9 – Comparison of predicted and test stress–strain response.

5. Conclusions

The uniaxial compressive performance of GFRP tube encased recycled concrete treated with nanoparticles were presented in this paper. The related conclusions can be drawn as following:

(1) The admixture of nanoSiO_2 and nano$CaCO_3$ in recycled concrete could improve the mechanical performance of untreated recycled concrete up to 1.2 times strength and 1.4 times strain.
(2) The GFRP encased recycled concrete treated with nanoparticles exhibited much higher compressive strength and better deformation ability than recycled concrete or GFRP encased untreated recycled concrete, the improvements on compressive strength of recycled concrete were around 49.6%–76.2% and the ductility indexes were about 5.38–8.48 times than that recycled concrete.
(3) The compressive strength of GFRP encased recycled concrete treated with nanoSiO_2 increased with an increasing dosage of nanoSiO_2 (up to 2 wt.%). And GFRP-NSRC with the mixing method II presented higher compressive than that with the mixing method I.
(4) The compressive strength of GFRP encased recycled concrete treated with nano$CaCO_3$ performed opposite trend to that of GFRP-NSRC which decreased with an increasing dosage of nano$CaCO_3$. And GFRP-NCRC performed better with the mixing method I.
(5) The reduced replacement rates of RCAs and increased of GFRP tube thickness exhibited positive influence on the strength and ultimate deformation of GFRP encased recycled concrete treated with nanoparticles.
(6) The same model used in FRP encased concrete could be also applied in simulating the ultimate behavior and stress–strain response of FRP encased recycled concrete treated with nanoparticles.

Declaration of Competing Interest

The authors declare no conflict of interest.

Acknowledgement

The research was financially supported by National Key Research and Development Program of China (2017YFC0703300) and by Bundesministerium für Bildung und Forschung (BMBF, Federal Ministry of Education and Research of Germany; Grant No.: 031B0914A). The gratitude would be extended to anonymous reviewers for their constructive comments during the review process. The authors acknowledge support by the German Research Foundation and the Open Access Publication Funds of the Technische Universität Braunschweig.

REFERENCES

[1] Ajayi Saheed O, Oyedele Lukumon O, Bilal Muhammad, Akinade Olugbenga O, Alaka Hafiz A, Owolabi Hakeem A, et al. Waste effectiveness of the construction industry: understanding the impediments and requisites for improvements. Resour Conserv Recycl 2015;102:101–12.
[2] Tang Z, Li W, Yan L. Mechanical behaviors of CFRP-confined sustainable geopolymer recycled aggregate concrete under both static and cyclic compressions 2020;252:112750.
[3] Gao C, Huang L, Yan L, Jin R, Chen H. Mechanical properties of recycled aggregate concrete modified by nano-particles. Constr Build Mater 2020;241:118030.
[4] Wang B, Yan LB, Fu QN, Kasal B. A comprehensive review on recycled aggregate and recycled aggregate concrete. Resour Conserv Recycl 2021;171:105565.
[5] Xiao JZ, Li WG, Fan YH, Huang X. An overview of study on recycled aggregate concrete in China (1996–2011). Constr Build Mater 2012;31:364–83.
[6] Chen W, Jin R, Xu Y, Wanatowski D, Li B, Yan LB, et al. Adopting recycled aggregates as sustainable construction materials: a review of the scientific literature. Constr Build Mater 2019;218:483–96.
[7] Wijayasundara M, Mendis P, Crawford RH. Methodology for the integrated assessment on the use of recycled concrete aggregate replacing natural aggregate in structural concrete. J Clean Prod 2017;166(10):321–34.
[8] Yehia Sherif, Kareem Helal, Abusharkh Anaam, Zaher Amani, Istaitiyeh Hiba. Strength and durability evaluation of recycled aggregate concrete. Int J Concr Struct Mater 2015;9(2):219–39.
[9] Silva RV, de Brito J, Dhir RK. Fresh-state performance of recycled aggregate concrete: a review. Constr Build Mater 2018;178:19–31.
[10] Tam VVWY, Kotrayothar D, Xiao JZ. Long-term deformation behaviour of recycled aggregate concrete. Constr Build Mater 2015;100:262–72.
[11] Shi CJ, Li YK, Zhang JK, Li WG, Chong LL, Xie ZB. Performance enhancement of recycled concrete aggregate-A review. J Clean Prod 2016;112(Part 1):466–72.
[12] Tošić Nikola, Marinković Snežana, Dašić Tina, Stanić Miloš. Multicriteria optimization of natural and recycled aggregate concrete for structural use. J Clean Prod 2015;87:766–76.
[13] Leite MB, Monteiro PJM. Microstructural analysis of recycled concrete using X-ray microtomography. Cement Concr Res 2016;81:38–48.
[14] Li WG, Xiao JZ, Sun ZH, Kawashima S, Shah Surendra P. Interfacial transition zones in recycled aggregate concrete with different mixing approaches. Constr Build Mater 2012;35:1045–55.
[15] Ryu JS. Improvement on strength and impermeability of recycled concrete made from crushed concrete coarse aggregate. J Mater Sci Lett 2002;21:1565–7.
[16] Akçaoğlu T, Tokyay M, Çelik T. Influence of interfacial transition zone on engineering properties of the concrete manufactured with recycled ceramic aggregate. J Civil Eng Manag 2015;21(1):358–63.
[17] Sáez del Bosquea IF, Zhu W, Howind T, Matías A, Sánchez de Rojas MI, Medina C. Properties of interfacial transition zones (ITZs) in concrete containing recycled mixed aggregate. Cement Concr Compos 2017;81:83–93.
[18] Tam VWY, Tam CM. Assessment of durability of recycled aggregate concrete produced by two-stage mixing approach. J Mater Sci 2007;42(10):3592–602.
[19] Tam VWY, Gao XF, Tam CM. Comparing performance of modified two-stage mixing approach for producing recycled aggregate concrete. Mag Concr Res 2006;58(7):477–84.

[20] Tam VWY, Tam CM. Diversifying two-stage mixing approach (TSMA) for recycled aggregate concrete: TSMAs and TSMAsc. Constr Build Mater 2008;22(10):2067–77.
[21] Li LG, Zhu J, Huang ZH, Kwan AKH, Li LJ. Combined effects of micro-silica and nano-silica on durability of mortar. Constr Build Mater 2017;157:337–47.
[22] Bibhuti BM, Sudhirkumar VB. Influence of Nano-Silica on the properties of recycled aggregate concrete. Constr Build Mater 2014;55:29–37.
[23] Berndt ML. Properties of sustainable concrete containing fly ash, slag and recycled concrete aggregate. Constr Build Mater 2009;23:2606–13.
[24] Shaikh FUA, Supit SWM, Sarker PK. A study on the effect of nano silica on compressive strength of high volume fly ash mortars and concretes. Mater Des 2014;60:433–42.
[25] Li W, Huang Z, Cao F, Sun Z, Shah SP. Effects of nano-silica and nano-limestone on flowability and mechanical properties of ultra-high-performance concrete matrix. Constr Build Mater 2015;95:366–74.
[26] Mohseni E, Naseri F, Amjadi R, Khotbehsara MM, Ranjbar MM. Microstructure and durability properties of cement mortars containing nano-TiO_2 and rice husk ash. Constr Build Mater 2016;114:656–64.
[27] Shiho K, Jung-Woo TS, Corr D, Hersam Mark C, Shah Surendra P. Dispersion of $CaCO_3$ nanoparticles by sonication and surfactant treatment for application in fly ash-cement systems. Mater Struct 2014;47:1011–23.
[28] Camacho María del Carmen, Galao Oscar, Javier Baeza Francisco, Zornoza Emilio, Garcés Pedro. Mechanical properties and durability of CNT cement composites. Materials 2014;7(3):1640–51.
[29] Bharj J. Experimental study on compressive strength of cement-CNT composite paste. Indian J Pure Appl Phys 2015;52(1):35–8.
[30] Kima HK, Park IS, Lee HK. Improved piezoresistive sensitivity and stability of CNT/cement mortar composites with low water-binder ratio. Compos Struct 2014;116:713–9.
[31] Xiao J, Li WG, Corr DJ, Shah SP. Effects of interfacial transition zones on the stress-strain behavior of modeled recycled aggregate concrete. Cem Concr Res 2013;52:82–99.
[32] Xiao J, Li WG, Sun ZH, Lange DA, Shah SP. Properties of interfacial transition zones in recycled aggregate concrete tested by nanoindentation. Cem Concr Res 2013;(37):276–92.
[33] Lim JC, Ozbakkaloglu T. Influence of silica fume on stress-strain behavior of FRP-confined HSC. Constr Build Mater 2014;63:11–24.
[34] Li WG, Huang Z, Zu T, Shi C, Duan W, Shah SP. Influence of nanolimestone on the hydration, mechanical strength, and autogenous shrinkage of ultra high performance concrete. J Mater Civ Eng 2015;28(1):315–23.
[35] Li WG, Long C, Tam VVWY, Poon CS, Duan WH. Effects of nano-particles on failure process and microstructural properties of recycled aggregate concrete. Constr Build Mater 2017;142:42–50.
[36] Bibhuti BM, Barai SV. Influence of Nano-Silica on the properties of recycled aggregate concrete. Constr Build Mater 2014;55:29–37.
[37] Ali Ahmed M, Masmoudi Radhouane. Experimental and analytical investigation of new concrete filled FRP tube beam-column connections. Eng Struct 2019;191:311–22.
[38] Huang L, Gao C, Yan L, Kasal B, Ma G, Tan H. Confinement models of GFRP-confined concrete: statistical analysis and unified stress-strain models. J Reinforc Plast Compos 2016;35(11):867–91.
[39] Huang L, Gao C, Yan L, Kasal B, Ma G. Reliability assessment of confinement models of carbon fiber reinforced polymer-confined concrete. J Reinforc Plast Compos 2016;35(12):996–1026.
[40] Huang L, Gao C, Yan L, Yu T, Kasal B. Experimental and numerical studies of CFRP tube and steel spiral dual confined concrete composite columns under axial impact loading. Compos B Eng 2018;152:193–208.
[41] Gao C, Huang L, Yan L, Ma G, Xu L. Compressive behavior of CFFT with inner steel wire mesh. Compos Struct 2015;133:322–30.
[42] Huang L, Xun X, Yan L, Zhu D. Compressive behavior of concrete confined with GFRP tubes and steel spirals. Polymers 2015;7(5):851–75.
[43] Yin P, Huang L, Yan L, Zhu D. Compressive behavior of concrete confined by CFRP and transverse spiral reinforcement. Part A: experimental study. Mater Struct 2016;49(3):1001–11.
[44] Xie T, Ozbakkaloglu T. Behavior of recycled aggregate concrete-filled basalt and carbon FRP tubes. Constr Build Mater 2016;105:132–43.
[45] Yan B, Huang L, Yan LB, Gao C, Kasal B. Behavior of flax FRP tube encased recycled aggregate concrete with clay brick aggregate. Constr Build Mater 2017;136:265–76.
[46] Gao C, Huang L, Yan LB, Jin RY, Kasal B. Strength and ductility improvement of recycled aggregate concrete by polyester FRP-PVC tube confinement. Compos B Eng 2019;162:178–97.
[47] Huang L, Yang X, Yan L, He K, Li H, Du Y. Experimental study of polyester fiber-reinforced polymer confined concrete cylinders. Textil Res J 2016;86(15):1606–15.
[48] Huang L, Chen L, Yan L. Behavior of polyester FRP tube encased recycled aggregate concrete with recycled clay brick aggregate: size and slenderness ratio effects. Constr Build Mater 2017;154:123–36.
[49] Gao C, Huang L, Yan L, Kasal B, Li W. Behavior of glass and carbon FRP tube encased recycled aggregate concrete with recycled clay brick aggregate. Compos Struct 2016;155:245–54.
[50] Tang Z, Li W, Tam VWY. Mechanical performance of CFRP-confined sustainable geopolymeric recycled concrete under axial compression. Eng Struct 2020;224:111246.
[51] GB/T 25177-2010. Recycled coarse aggregate for concrete. Standardization Administration of The People's Republic of China; 2011.
[52] D. ASTM. Standard test method for tensile properties of polymer matrix composite materials. 2008.
[53] Pour AF, Ozbakkaloglu T, Vincent T. Simplified design-oriented axial stress-strain model for FRP-confined normal- and high-strength concrete. Eng Struct 2018;175:501–16.
[54] Zeng YH, Botte W, Caspeele R. Reliability analysis of FRP strengthened RC beams considering compressive membrane action. Constr Build Mater 2018;169:473–88.
[55] Jin RY, Yan LB, Soboyejo ABO, Huang L, Kasal B. Multivariate regression models in estimating the behavior of FRP tube encased recycled aggregate concrete. Constr Build Mater 2018;191:216–27.
[56] Li YL, Teng JG, Zhao XL, Singh Raman RK. Theoretical model for seawater and sea sand concrete-filled circular FRP tubular stub columns under axial compression. Eng Struct 2018;160:71–84.
[57] Zhou YW, Liu XM, Xing F, Cui HZ, Sui LL. Axial compressive behavior of FRP-confined lightweight aggregate concrete: an experimental study and stress-strain relation model. Constr Build Mater 2016;119:1–15.
[58] Henni ID, Kassoul A. Stress-strain model of confined concrete with Aramid FRP wraps. Constr Build Mater 2018;186:1016–30.
[59] Lam L, Teng J. Design-oriented stress-strain model for FRP-confined concrete. Constr Build Mater 2003; 17:471–89.